The paper was published in the proceedings of the 11th International Conference on Physical Modelling in Geotechnics (ICPMG2026) and was edited by Ioannis Anastasopoulos. The conference was held from June 8th to June 12th 2026 in Zurich, Switzerland.

Proceedings of the 11th ICPMG 2026
11th International Conference on Physical Modelling in Geotechnics
8-12 June 2026, Zurich, Switzerland

Stress wave analysis of monopile driving in sand informed by embedded fibre Bragg grating sensors

M.E. Rasmussen
University of Oxford, Oxford, UK, magne.rasmussen@eng.ox.ac.uk

V. Nardelli, H.J. Burd, B.W. Byrne
University of Oxford, Oxford, UK

R.M. Buckley
University of Glasgow, Glasgow, UK

R. Keane
Geowynd, Southampton, UK (formerly University of Oxford, Oxford, UK)

ABSTRACT: Stress wave propagation in monopiles during driving is conventionally analysed using Pile Driving Analyzer (PDA) sensors mounted at the pile head. PDA acceleration measurements can be interpreted through one-dimensional stress wave theory and signal matching techniques. However, the limited spatial resolution of the PDA measurements leads to non-unique solutions, resulting in interpretations of the distributed shaft and base resistances that are inevitably subjective. The PICASO (PIle Cyclic AnalySis: Oxford and Ørsted) joint industry and research project enabled the acquisition of high-resolution strain data along the embedded length of medium-scale field test piles by incorporating below-ground optical fibre Bragg grating (FBG) sensors as part of the instrumentation. Using a hybrid PDA and FBG signal matching approach, proven and validated in previous studies, this paper reports on applications of stress wave propagation analysis for pile driving in homogeneous silica sand. The enhanced PICASO field data from both PDA and FBG sensors significantly constrain the stress wave solution space, yielding insights into the development of soil resistance to driving, a critical factor for accurate driveability predictions. The obtained hybrid signal matching results are compared with the shaft and base resistances predicted using a well-known empirical method.

1 INTRODUCTION

Large-diameter, open-ended monopiles are a common foundation solution for offshore wind and near-shore structures. The piles are typically driven into the seabed using impact hammers. Successful installation depends on pile driveability assessments to select appropriate hammer type and settings such that the required penetration depth is achieved without inducing excessive pile stresses.

Evaluating pile driveability requires knowledge of the soil resistance to driving (SRD). SRD is commonly estimated using empirical formulas that relate in situ measurements to soil resistance, with the Alm and Hamre (2001) method widely adopted in the industry. To complement the empirical methods with higher-fidelity analyses, stress wave propagation along the pile during driving can be examined either in real-time or through post-installation data analysis. This more mechanistic SRD assessment involves monitoring piles dynamically during driving.

Traditionally, the monitoring consists of above-ground strain and velocity signals from a Pile Driving Analyzer (PDA) system. Signal matching techniques applied to these two signals determine the distribution of shaft and base resistances along the pile, from which the axial pile capacity is inferred.

The PICASO (PIle Cyclic AnalySis: Oxford and Ørsted) joint industry and research project investigates the effects of lateral cyclic loading and loading rate on monopile behaviour. The project outcomes are benchmarked against two medium-scale field test campaigns at different sites. One of these campaigns was conducted in medium-dense to dense silica sand at a PICASO test site in Cuxhaven, Germany (Byrne et al., 2025a). A total of 25 tubular steel piles (12 test piles and 13 reaction piles) were installed. During pile driving, most test piles were instrumented with optical fibre Bragg grating (FBG) sensors for strain and temperature measurements recorded at 5 kHz. In addition, a subset of test piles was equipped with PDA sensors recording at a higher sampling rate of 40 kHz.

The high-resolution FBG recordings during installation at the sand site offer improvements to the mechanistic SRD assessment by allowing tracking of the stress wave propagation along the pile, enhancing the spatial understanding of the stress wave and thus the resistances. Buckley et al. (2020) introduced a hybrid signal matching approach that uses optical FBG recordings to constrain the SRD solution space. This paper extends the method to a test site with a different soil profile focusing on homogeneous sand, and, along with the work by Martin et al. (2022) for an overconsolidated glacial till, it validates the method by Alm and Hamre (2001) for the PICASO test piles.

2 SITE DESCRIPTION

The PICASO project consisted of two substantial pile testing campaigns at two different sites. The first of the two was performed at Cowden (UK), where the ground conditions consisted of overconsolidated glacial till (Martin et al., 2022), whereas the second was carried out at Cuxhaven (Germany), at a site characterised by the presence of medium-dense to dense silica sand (Byrne et al., 2025b). Both sites were selected to perform testing at ground conditions representative of those typically encountered in the North Sea, where a significant number of wind farms have been built in the past decades. This study refers to the pile testing campaign developed at the sand site in Cuxhaven.

The Cuxhaven area lies in the North German Plain, whose coasts are bounded by the North Sea. The main shallow formation in the area is constituted by Pleistocene North Sea clean sands, which are deltaic sediments deposited in the German Bight during inter-glacial periods (Knudsen et al., 2019). The site selected for pile testing was characterised after performing a comprehensive site investigation campaign, which consisted of 7 boreholes, 27 cone penetrometer tests (CPTs) and 4 seismic cone penetrometer tests (SCPTs), among others. From the analysis of the ground investigation data, the presence of medium-dense to dense homogeneous silica sands for the first 10 m was recorded for the whole site area, with a very occasional presence of lenses of silty sands and gravelly sands. Higher presence of gravelly sands was recorded for depths greater than 10 m, which had no impact on pile installation and testing considering the pile toe depths.

Figure 1a shows the profiles of minimum, maximum and average corrected cone resistances q_t obtained from the CPTs performed on site against the reduced level (RL) in m NHN (Normalhöhennull,

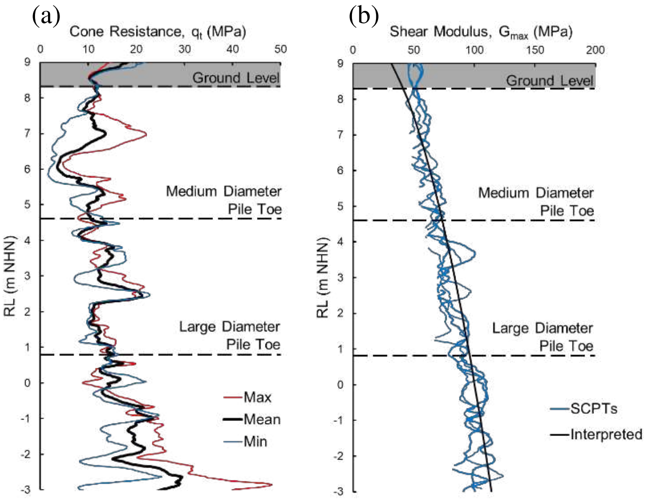

Figure 1. Profiles of a) CPT cone resistance q_t with depth; b) small-strain shear modulus G_{max} data with depth.

reference system used in Germany). Figure 1b reports the interpreted trend of the small-strain shear modulus G_{max} with depth, which has been inferred using the expression proposed by Hardin (1978) from the measurements of shear wave velocities from the SCPTs and the correlation proposed by Rix and Stokoe (1992) using the cone resistances recorded during the tests.

3 PILE DRIVING INSTRUMENTATION

11 test piles instrumented with FBGs were installed for the PICASO testing campaign at Cuxhaven. Of these piles, the installation of 10 was performed by impact driving and 1 was installed by vibratory methods. Four piles were also equipped with Pile Driving Analyzer (PDA) sensors. The geometries of the piles tested at Cuxhaven, along with the configuration of the FBGs and PDAs installed, are shown in Figure 2.

Vertical arrays of 16 FBG gauges (large-diameter piles) or 17 gauges (small-diameter piles) were installed in 5mm square channels on the exterior pile wall. Each pile was instrumented with two or four arrays, and strain readings from all gauges at each level were averaged. PDA recordings were performed at a single location with 2 averaged readings per pile.

Of the 11 piles installed, 3 had large diameter (D=2.5 m, thickness t=36 mm and steel grade S355) and 8 had medium diameter (D=1.22 m, steel grade S420). The thickness of medium piles was t=13 mm except for one, which had thickness t=16 mm. The large diameter piles were all equipped with FBGs and PDAs and were installed using the hydraulic hammer IQIP IHC S150. Of the medium diameter piles, 8 were equipped with FBGs and 1 was equipped with PDAs

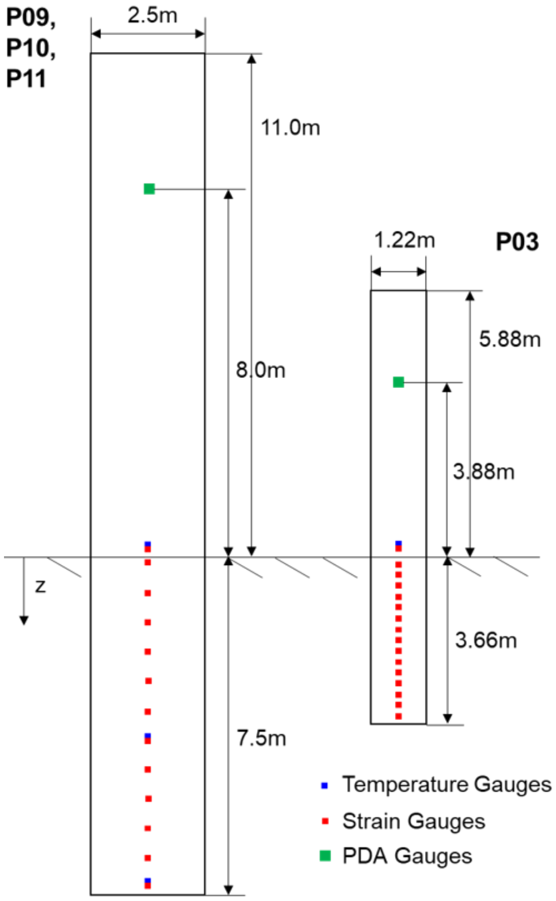

Figure 2. Pile geometries and layout of FBG temperature gauges (blue markers), FBG strain gauges (red markers), and PDA gauges (green markers). z is depth below ground level (positive downward).

during its installation. Their installation was also performed using a hydraulic hammer IQIP IHC S150, except for one pile that was vibrated using a hammer Dieseko ICE 28RF. All piles were installed reaching a toe depth of 3 times the diameter D, and a final height H of 4D plus 1 m to accommodate the installation of the equipment required for testing them laterally.

Figures 3a and 3b show the blow count profiles recorded for every 250 mm of driving for the large diameter (a) and the medium diameter (b) piles during their installation. It can be observed that the data recorded are fairly consistent, especially for the large piles. Regarding the medium diameter piles, relatively low resistance was recorded towards the end of the installation of P05.

4 MEASUREMENTS DURING DRIVING

To achieve a mechanistic SRD assessment, the stress wave propagation induced by hammer blows can be modelled using a one-dimensional wave equation. Several numerical methods exist for solving the wave

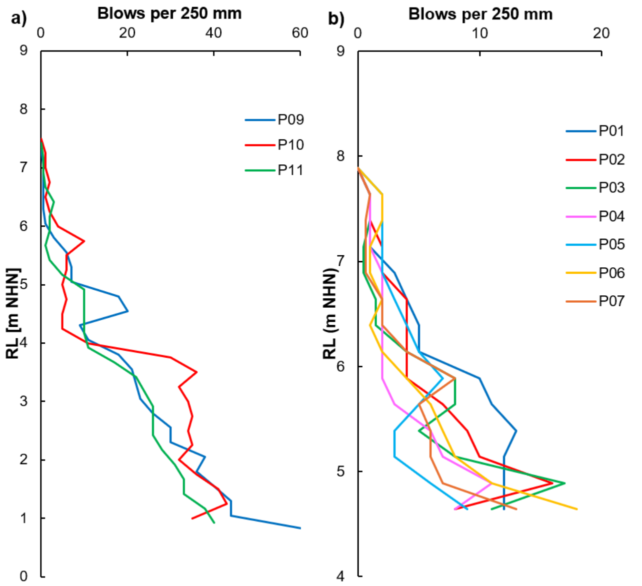

Figure 3. Blow counts recorded during pile installation for a) large diameter piles and b) medium diameter piles.

equation, including finite difference schemes with explicit or implicit time integration and finite element formulations (Randolph, 2008). The signal matching method adopted in this paper seeks to eliminate the need for explicit hammer modelling. It builds on characteristic solutions, w, of the wave equation of the form:

$$w(z,t) = f_{dn}(z - ct) + f_{up}(z + ct) \quad (1)$$

where w is the axial displacement and c is the wave propagation speed in the material. f_{dn} and f_{up} represent downward (increasing z) and upward travelling displacement wave functions, respectively. Taking spatial and temporal derivatives of w yields expressions for axial force and particle velocity:

$$F = -E\,A\,(f'_{dn} + f'_{up}) \quad (2)$$
$$v = -c\,(f'_{dn} - f'_{up}) \quad (3)$$

where E is Young's modulus, A is the cross-sectional area, and primes denote differentiation with respect to the wave argument. Introducing the pile impedance $Z = EA/c$ couples Eqs. 2 and 3, allowing the downwards and upwards travelling forces to be determined by:

$$F_{dn} = \frac{F+Zv}{2}, \quad F_{up} = \frac{F-Zv}{2} \quad (4)$$

Field measurements of F and v enable the identification of the two travelling force signals, which is the minimal requirement for signal matching.

4.1 PDA measurements

To support stress wave analysis during pile driving, the PDA measured accelerations following each hammer blow can be integrated to provide velocities v. Both Young's Modulus, E, of the steel pile and the cross-sectional area, A, are known parameters, allowing the pile impedance to be calculated.

Measurements of strain ε are used to calculate the axial force $F = EA\varepsilon$. In practice, the peak force was measured to be 3-8% lower than the peak Zv. The measurement of acceleration was considered to be more reliable, so the force signal was multiplied by a factor of $(Zv)_{peak}/F_{peak}$. This resulted in upwards travelling wave forces of approximately zero before the first reflection, except for minor instrument noise.

4.2 FBG measurements

The FBG readings of strain are also converted to axial force using $F = EA\varepsilon$. This is done for all vertical levels, resulting in a spatial and temporal distribution of axial forces. While PDA-measured F and Zv values returned to near-zero after each hammer strike, FBG sensors typically recorded residual non-zero values at blow completion. The residual strain and thus axial forces tended to increase with continued driving. Observations of increasing residual forces were also recorded by Buckley et al. (2020) and Martin et al. (2022). Because the individual effects of temperature, steel stress, and sand shaft friction on these residual forces could not be reliably separated, strain gauges were re-zeroed at each blow to streamline the analysis.

Figure 4 compares forces calculated from above-ground FBG strain gauges (gauge series 02) with PDA measurements taken 7.85 m above the FBG gauges for blow 112, pile P09. Comparable values in peak forces are achieved prior to any wave reversals.

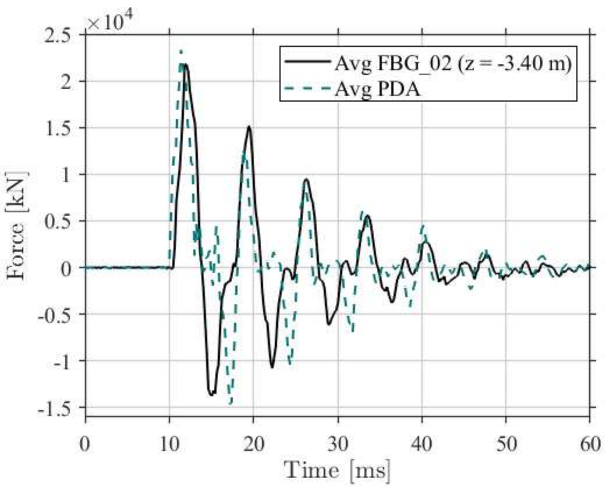

Figure 4. Force measurements from PDA and above ground FBG strain gauges for pile P09 blow 112.

5 STRESS WAVE ANALYSIS

Stress wave analysis was performed for a variety of different blows for the four piles with PDA recordings during driving. This paper will focus on four blows during the driving of Pile P09. The selected blows and corresponding estimated embedment depths are 50 (3.5 m), 112 (4.25 m), 405 (6.90 m) and 508 (7.46 m). A total of 518 blows were performed during the installation, reaching a total embedment of 7.5 m.

The software IMPACT version 4.2 (Randolph, 2008) was used for the stress wave interpretation of dynamic measurements. IMPACT evaluates pile response using shaft and toe resistance formulations derived from elasto-dynamic theory (Deeks and Randolph, 1995; Simons and Randolph, 1985).

For each hammer blow, the downward travelling force, $\mathrm{F_{dn}}$, is taken as a known input and is imposed at the pile head. Using assumed values of shaft and base resistance, IMPACT estimates the corresponding upwards travelling wave $\mathrm{F_{up}}$. The estimated $\mathrm{F_{up}}$ is then compared with the measured $\mathrm{F_{up}}$ through signal matching, which allows the pile resistance parameters to be iteratively adjusted until an acceptable match is achieved.

5.1 Input parameters

The sand density ρ and shear modulus G were determined from the PICASO sand site investigation. The shear modulus was taken directly from the small-strain profile G_{max} presented in Figure 1(b).

A preliminary ultimate end-bearing pressure q_b was derived from CPT data obtained at the location of pile P09, using the expression for unit tip resistance for sands proposed by Alm and Hamre (2001):

$$q_b = 0.15 \times q_t \times (q_t/\sigma_v')^{0.2} \tag{5}$$

No independent sensors or tests were available to validate the unit tip resistance found using Eq. (5). To account for potential uncertainty associated with the empirical formulation, q_b was therefore treated as a variable input parameter in the IMPACT software.

The pile-specific CPT sleeve friction profile was used to estimate a preliminary shear stress profile. This distribution, together with q_b, was adopted as baseline input and subsequently adjusted through both manual and automated iterative procedures, as described in Section 5.2.

The piles were assumed to remain unplugged throughout driving, with soil resistance acting only on the external surface area. Finally, the IMPACT software viscous interaction parameters $\alpha = 1, \beta = 0.2$ were fixed as recommended by Randolph (2008).

5.2 Optimisation procedure

Three signal-matching procedures were assessed, each involving iterative variation of the shear stress profile and end-bearing pressure:

a) manual signal matching
b) automated PDA only - optimisation
c) automated PDA-FBG – optimisation

The manual procedure (a) was adopted first. The preliminary shear stress profile and end-bearing pressure were adjusted incrementally at different pile horizons, with each modification evaluated using two error metrics: ζ_h, ζ. ζ_h represents the normalised error at the pile head based on the PDA signal:

$$\zeta_h(\%) = \left(\frac{\zeta_{f,up}}{F_{up,max}}\right) \quad (6)$$

Where, for a given blow, $\zeta_{f,up}$ is the average root mean square error between measured and calculated upward wave force. $F_{up,max}$ is the maximum upward force at the pile head.

ζ represents a weighted total error using both the PDA signal at the pile head and FBG signals along the pile:

$$\zeta(\%) = \frac{0.5}{n} \times \sum_{i=1}^{n} \frac{\zeta_f(i)}{F_{max}(i)} + 0.5\left(\frac{\zeta_{f,up}}{F_{up,max}}\right) \quad (7)$$

where n is the number of strain gauge horizons. For a given blow, ζ_f is the average root mean square error between the measured and calculated impact force. F_{max} is the maximum impact force.

The shear stress profile obtained from manual signal matching was then used as the initial input for the automated optimisation procedures (b) and (c).

Procedure (b) assumed the PDA measurements were the only available signal and therefore minimised Eq. 6. However, this conventional approach suffers from non-unique solutions within an otherwise flat optimisation landscape, which consequently leads to subjectivity in parameter selection (Fellenius, 1988).

To address this limitation, Buckley et al. (2020) proposed matching calculated force signals at multiple pile depths with FBG measurements, thereby further constraining the signal matching process. This was adopted in procedure (c), which minimised Eq. 7 as the objective function. The associated MATLAB code from Buckley et al. (2020) has been further developed for use with the PICASO piles and instrumentation.

5.3 Treatment of PDA signal noise

Reliable signal matching results require high-quality force and velocity signals. One way to assess signal quality is to examine the upward-travelling force, F_{up}, in the time interval in which the wave propagates along the free stick-up length of the pile, where it should ideally be zero (Buckley et al., 2020). In Figure 5, the PDA signal shows irregular fluctuations about zero prior to the arrival of the first reflected wave. This behaviour was observed across all blows, most notably at shallow embedment, suggesting that the instruments may not have been properly fixed to the pile.

To minimise the impact of PDA noise during optimisation, the otherwise global optimisation was carried out sequentially, with the tip resistance, q_b, optimised first. The shear stress profile was further constrained within the bounds $0 < \tau < 250$ kPa.

5.4 Signal matching results

Figure 5 presents the measured upwards travelling wave force at the pile head and the corresponding pile head displacement for the deep blow 508 during the

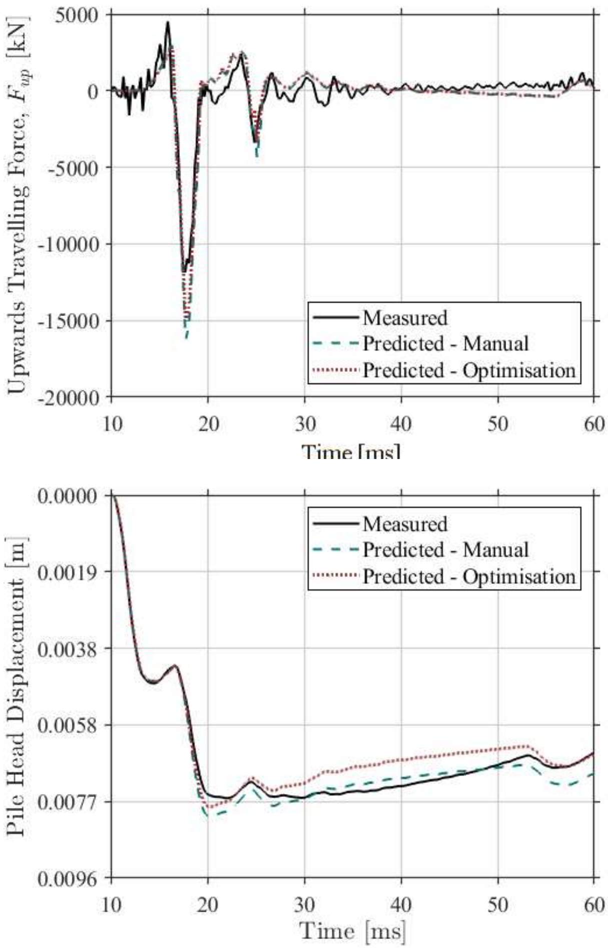

Figure 5. Comparison of upwards travelling wave force and displacement obtained from manual and PDA-FBG optimisation-based signal-matching methods with PDA measurements recorded during blow 508, Pile P09.

installation of pile P09. The manual and PDA-FBG optimised predictions are also shown. Reasonable agreement is achieved between the measured and IMPACT upward travelling waves. The optimised predictions show slight improvement over the manual solution in the early stage by better matching the first peaks of the upward travelling force.

The corresponding error metrics for blow 508 are reported in Table 1, which demonstrate the percentage improvement achieved by an optimisation scheme. The optimisation procedures (b) and (c) provide modest but consistent improvements to the manual procedure (a), both at the pile head (ζ_h) and in terms of the total error (ζ).

Generally, the PDA-only optimisation procedure (b) and the hybrid optimisation procedure (c) achieve similar accuracies at the pile head. However, the hybrid signal matching approach outperforms the PDA-only optimisation in terms of the total error, ζ. This behaviour reflects the non-unique wave equation solution issues highlighted by Fellenius (1988).

Table 1 – Comparison of normalised error obtained by manual signal matching and optimisation. ζ_h is the error at pile head, Eq. 6, and ζ is the PDA-FBG weighted, Eq. 7.

Blow No.	**(a) Manual**		**(b) PDA only Optimisation**		**(c) PDA-FBG Optimisation**	
	ζ_h (%)	ζ (%)	ζ_h (%)	ζ (%)	ζ_h (%)	ζ (%)
50	6.5	8.7	6.1	8.5	6.2	8.4
112	5.2	6.9	4.7	6.6	4.8	6.4
405	5.2	4.9	4.7	4.7	4.9	4.5
508	5.3	5.0	5.0	4.9	5.1	4.6

Figure 6 shows the measured and calculated force time histories at selected FBG strain gauge horizons along the embedded pile length for one of the final blows, blow 508. For this particular blow, the PDA-FBG optimisation does not change the predicted impact forces significantly. Both procedures consistently overpredict the peak impact forces, particularly for FBG measurements located near the pile toe. A similar result was observed at the clay site (Martin et al, 2022).

Each of the three signal-matching procedures involved iterative adjustment of the shear stress profile. The final shear stress profiles obtained from each procedure can be used to compute corresponding mobilised shear stress. Distributions of mobilised shear stresses using (c) are shown in Figure 6.

6 SOIL RESISTANCE TO DRIVING

The optimised mobilised shear stress profiles provide a mechanistically informed estimate of the major

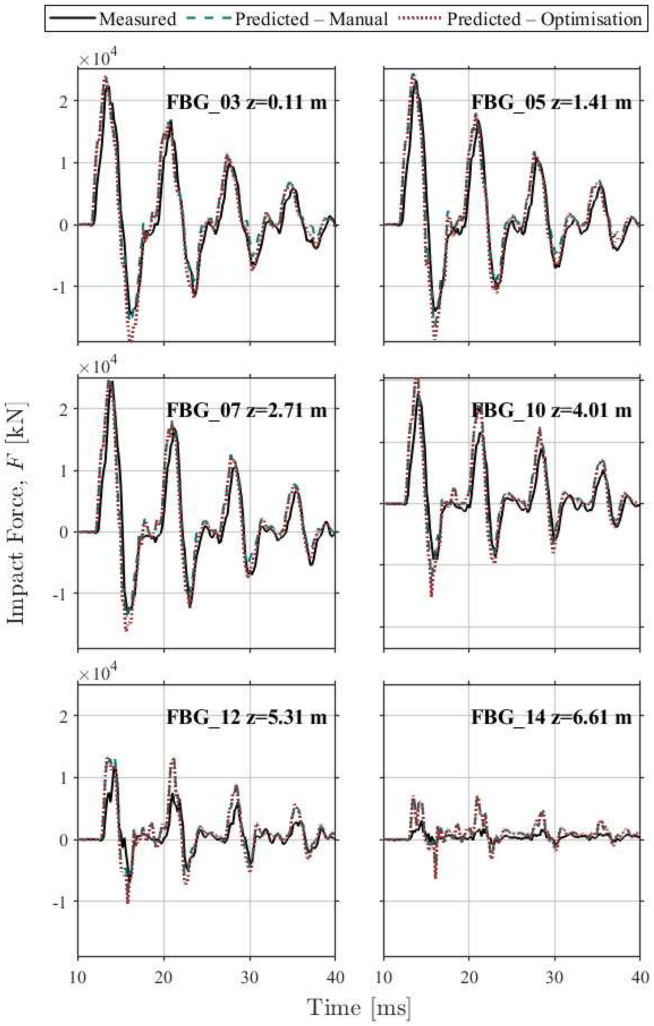

Figure 6. Measured and predicted impact forces at six FBG gauge depths for pile P09, blow 508, comparing conventional manual signal matching with the hybrid PDA-FBG optimisation approach.

contribution to SRD, i.e. side friction. Another approach is the method introduced by Alm and Hamre (2001), which establishes analytical relationships between cone tip resistance and SRD. It is built upon an exponential degradation of friction (friction fatigue), where the mobilised shear stresses at any given soil horizon reduce as the pile is driven further.

Alm and Hamre (2001) observed from their database that the CPT-based method slightly overpredicts resistance during driving, resulting in conservative estimates of driveability. Mobilised shaft resistance calculated using this method and CPT data from the P09 location was compared with results from PDA–FBG optimisations performed in IMPACT, as shown in Figure 7.

Good agreement is found between the two approaches for the two shallower blows, and the Alm and Hamre method remains consistently conservative. However, for the two deeper blows, the mechanistic signal-matching approach produced shear stress profiles characterised by high stresses near the ground surface. This pronounced initial mobilisation of shaft resistance predicted by the IMPACT calculations, combined with the found limited effects of friction fatigue during driving at the Cuxhaven sand site, indicates that the Alm and Hamre method may lead to unconservative estimates under these conditions.

The driveability analysis results are consistent with observations reported by Kourelis et al. (2022), who found that the Alm and Hamre method tends to underpredict blow counts in sand layers at increasing embedment depths, based on driving records from 6.5 m diameter monopiles installed in the North Sea.

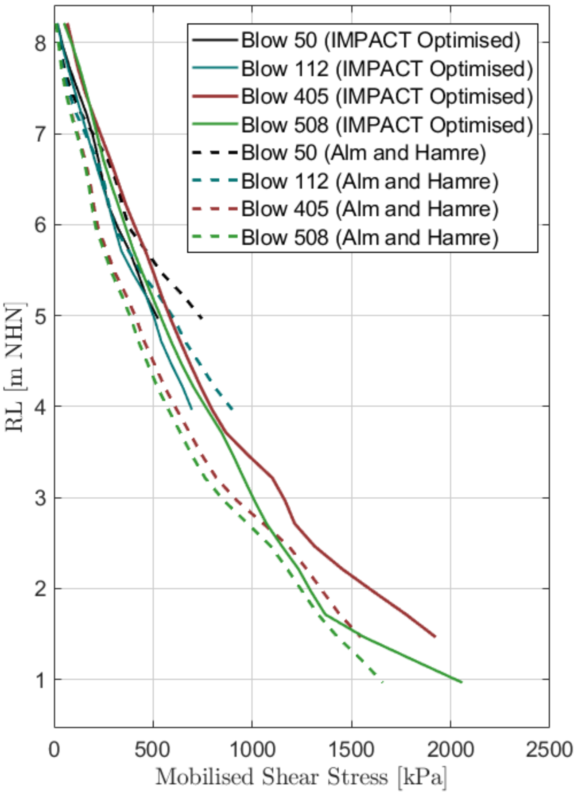

Figure 7. Comparison of mobilised shaft resistance obtained from signal-matching optimisation with the Alm and Hamre (2001) CPT-based correlation.

7 LIMITATIONS

The PDA field data exhibited elevated noise levels, particularly for the two shallower blows, blow 50 and 112. To mitigate this, the optimisation was carried out sequentially instead of at a global level and physically reasonable bounds were introduced for the shear stress profile. Future work could explore different weighting functions between instrument signals in the error metrics. The metrics ζ and ζ_h could also be defined over specified time intervals. The interpretation of friction fatigue effects is inferred from back-calculated resistance trends. Pore pressure accumulation between blows, as well as variations in transient dissipation during pile blows, could influence the back-calculated resistance trends. The present study does not account for the influence of excess pore pressure.

8 CONCLUSIONS

Stress wave analyses of monopile driving in homogeneous silica sand were performed using combined PDA and FBG measurements from the PICASO field test campaign at Cuxhaven. A novel signal matching procedure proposed by Buckley et al. (2020), reduced the non-uniqueness associated with conventional stress wave analysis by including below-ground strain data recorded by fibre Bragg gratings.

Compared to manual and PDA-only signal matching, the hybrid PDA–FBG method provided improved agreement between measured and predicted force histories along the pile for all studied blows. The improvements were modest, reflecting the sensitivity of the optimisation to the quality of the measured force and velocity input signals. The mobilised shaft resistance profiles obtained from the hybrid PDA–FBG method were broadly consistent with CPT-based predictions at shallow embedment but diverged at greater depths, showing a pronounced initial mobilisation and limited evidence of friction fatigue.

The results show that incorporating below-ground FBG measurements into stress wave analyses can improve confidence in soil resistance to driving estimates, supporting reliable driveability assessments for offshore wind monopile installations. The improvement of results achieved through the introduction of optimisation schemes depends on the quality of the measured force and velocity signals.

ACKNOWLEDGEMENTS

The authors acknowledge the support of Ørsted in funding the PICASO project. Also, the authors would like to thank Per Aarsleff for the pile installation at Cuxhaven, Marmota Engineering for providing the FBG instrumentation and GSP for the PDA instrumentation. Byrne is supported by the Royal Academy of Engineering under the Research Chairs and Senior Research Fellowships scheme.

REFERENCES

Alm, T. and Hamre, L. (2001). Soil model for pile driveability predictions based on CPT interpretations. Proceedings of the 15th International Conference on Soil

Mechanics and Geotechnical Engineering, Istanbul, Turkey, 2, pp. 1297-1302.

Buckley, R. M., McAdam, R. A., Byrne, B. W., Doherty, J. P., Jardine, R. J., Kontoe, S. and Randolph, M. F. (2020). Optimization of impact pile driving using optical fiber Bragg-grating measurements. Journal of Geotechnical and Geoenvironmental Engineering, Vol. 146 (9). https://doi.org/10.1061/(ASCE)GT.1943-5606.0002293

Byrne, B. W., Burd, H. J., Houlsby, G. T., Kamas, I., Keane, R., Malhotra, S., Martin, S. C., Nardelli, V., Qiu, Z. H., Rasmussen, M. E., Simonin, L., Saberi, M., Wen, K. Z., Wu, K. K., Buckley, R., Crispin, J. J., Shonberg, A., Soares Cunha, V. and Vaitkune, E. (2025a). PICASO: Cyclic loading of wind turbine monopiles. Proceedings of the 5th International Symposium on Frontiers in Offshore Geotechnics (ISFOG 2025), Nantes, France. https://doi.org/10.53243/ISFOG2025-506

Byrne, B. W., Burd, H. J., Houlsby, G. T., Keane, R., Nardelli, V., Rasmussen, M. E., Saberi, M., Buckley, R., Crispin, J., Cameron, A., Crook, A., Kragelund, J., Shonberg, A., Soares Cunha, V., Turner, S., Vaitkune, E. and Wen, K. (2025b). Cyclic loading of monopiles at a saturated dense sand site in Germany. Proceedings of the 5th International Symposium on Frontiers in Offshore Geotechnics (ISFOG 2025), Nantes, France. https://doi.org/10.53243/ISFOG2025-507

Deeks, A. J. and Randolph, M. F. (1995). A simple model for inelastic footing response to transient loading. International Journal for Numerical and Analytical Methods in Geomechanics, 19 (5), pp. 307–329. https://doi.org/10.1002/nag.1610190502

Fellenius, B. H. (1988). Variation of CAPWAP results as a function of the operator. Proceedings of the 3rd International Conference on the Application of Stress Wave Theory to Piles, Ottawa, pp. 814–825.

Hardin, B. O. (1978). The nature of stress–strain behaviour for soils. Proceedings of the ASCE Geotechnical Engineering Division speciality conference, Pasadena, CA, USA, Vol. 1, pp. 3–90.

Knudsen, S., Lunne, T., Quinteros, V.S., Vestgården, T. Krogh, L. and Bøgelund-Pedersen, R. (2019). Effect of reconstitution techniques on the triaxial stress-strength behaviour of a very dense sand. Proceedings of the XVII ECSMGE. https://doi.org/10.32075/17ECSMGE-2019-0575

Kourelis, I., Kontoe, S., Buckley, R. M. and Galbraith, A. (2022). An assessment of pile driveability analyses for monopile foundations. Proceedings of the 11th International Conference on Stress Wave Theory and Design and Testing Methods for Deep Foundations (SW2022), Rotterdam, The Netherlands. https://doi.org/10.5281/zenodo.7148969

Martin, S. C., Buckley, R. M., McAdam, R. A. and Byrne, B. W. (2022). Enhanced stress wave analysis of scaled monopiles in glacial till at Cowden. Proceedings of the 11th International Conference on Stress Wave Theory and Design and Testing Methods for Deep Foundations (SW2022), Rotterdam, The Netherlands. https://doi.org/10.5281/zenodo.7151557

Randolph, M. F. (2008). IMPACT—Dynamic analysis of pile driving. Crawley, Australia, Department of Civil and Environmental Engineering, University of Western Australia.

Rix, G. J. and Stokoe, K. H. (1992). Correlation of initial tangent modulus and cone resistance. Proceedings of the International Symposium on Calibration Chamber Testing, Potsdam, New York, USA, pp. 351–362.

Simons H. A. and Randolph, M. F. (1985). A new approach to one dimensional pile driving analysis. Proceedings of the International Conference on Numerical Methods in Geomechanics, Cambridge, UK, pp. 1457–1464.

.